Biointerface Research in Applied Chemistry
Open-Access Journal (ISSN: 2069-5837)

Article
Volume 14, Issue 3, 2024, 58
https://doi.org/10.33263/BRIAC143.058

Optimization on Characterization and Physicochemical of Non-Calcined and Calcined Nanocrystallite of Cuttlefish (*Sepia officinalis*) Bones Powder for Sustainable Green Technology Applications

Nurunabihah Aqilah Zulkarnain [1], Aima Ramli [1,2,*], Nurul Huda Abd Kadir [1,3,*]

1. Faculty of Science and Marine Environment, University Malaysia Terengganu, 21030 Kuala Nerus, Terengganu, Malaysia;
2. Advanced Nanomaterials Research Interest Group, Faculty of Science and Marine Environment, University Malaysia Terengganu, 21030 Kuala Nerus, Terengganu, Malaysia
3. Biological Security and Sustainability Research Interest Group, Faculty of Science and Marine Environment, University Malaysia Terengganu, 21030 Kuala Nerus, Terengganu, Malaysia

* Correspondence: aima.ramli@umt.edu.my (A.R), nurulhuda@umt.edu.my (N.H.A.K.),

Scopus Author ID 57191625830

Received: 10.07.2023; Accepted: 20.12.2023; Published: 4.02.2024

Abstract: Marine waste, including prawn skin, mollusk shells, and cuttlefish bones, contain inorganic compounds such as Calcium (Ca), Magnesium (Mg), Sodium (Na), Potassium (K), Rubidium (Rb), Barium (Ba) and Strontium (Sr), which is useful in green technology applications. Even though the characterization of cuttlefish bones has been reported, the characterization of the calcined cuttlefish bones requires more research. This study focused on the characterization and physicochemicals of non-calcined (NCB) and calcined-cuttlefish bones (CCB) (*Sepia Officinalis*) as potential for green technology. The structure and morphology of NCB and CCB were examined using TGA, SEM, XRD, and FTIR at the temperatures of 350°C, 700°C and 900°C. Based on the results, TGA analysis revealed that the structure of the CCB was gradually denatured at 600°C and destroyed at 700°C. SEM morphological structure of NCB and CCB revealed that the lamella structure of the materials at 350°C was remained in preserved structure at 350°C but diminished at 700°C and 900°C. Ca, Carbon (C), and Oxygen (O) are the main component elements that are abundant in NCB and CCB using SEM-EDX analysis. The crystallite size of the samples decreases with the increased time of calcination temperature, which results in polymorph change from orthorhombic to hexagonal, as depicted via XRD analysis. The XRD results have represented that the NCB and CCB crystallite size at temperatures of 0°C, 350°C, 700°C and 900°C were 55.52nm, 64.03nm, 44.74nm, and 23.30nm, respectively. Furthermore, FTIR analysis indicated that all the NCB and CCB samples were in aragonite and calcite polymorph form. While considering the summary of the study, it was revealed and observed that NCB and CCB could be potentially significant biomaterials in the field of green technology and its advanced applications in recent times. Furthermore, it is also important to mention that its remarkable properties, such as high stability and characterization, make it an ideal choice for a sustainable future.

Keywords: cuttlefish bones; calcined-cuttlefish bones; characterization; physicochemical.

1. Introduction

Sustainable materials such as chitosan from prawn skin and natural calcium carbonate ($CaCO_3$) from the cuttlefish bone [1] have been introduced for intended use in green technology [2], like in construction [1], wastewater treatment [3], medical purposes [4] and also to address

waste problems around the world. The marine waste, apart from other wastes, can also generate carbon dioxide (gas with high GWP) during the heating process (sun exposure) of organic compounds such as $CaCO_3$, which decompose into calcium ions and carbon dioxide. Research studies on marine waste have involved an increased number of researchers in the field of superconductors [5] driven by various elements, mostly in their shell or exoskeleton parts, which do not naturally decompose in water. Cuttlefish bone, a form of marine waste, comprises organic materials (3.0–4.5%) and $CaCO_3$ (Aragonite polymorph stabilized by Strontium) [6], while this waste can be found along the seashore.

As per the available literature, it is evident that the cuttlefish bone holds many potential capabilities as a doping agent that can be applied for future research [7]. Notably, cuttlefish bone has high porosity, flexural stiffness, and compressive strength, which position it as a viable biomaterial [8]. Moreover, its hard and agglomerate internal structure supports buoyancy, consisting of a dorsal shield (external region) and an internal lamellar region.

According to available research, the researchers identified the major elements of the cuttlefish bone, including calcium (Ca), carbon (C), oxygen (O), and a small amount of Sodium (Na), Magnesium (Mg), Potassium (K) and Strontium (Sr) [3]. In addition, Ca, C, and O were the most important elements present in the chemical structure of cuttlefish bone, along with a small percentage of sodium [6], potassium, and yttrium [9]. A study on morphological characterization of the cuttlefish bone has been carried out by Rial *et al*. [10], and their findings revealed that there are many possible shapes that can emerge during the calcination process. However, the calcination process of calcium carbonate involves exposing $CaCO_3$ to high temperatures to induce thermal decomposition. This process results in the formation of calcium oxide (CaO) and the release of carbon dioxide (CO_2) as a byproduct.

This study uses cuttlefish bone to determine element content, characterization, chemical properties, and its potential as natural calcium oxide for use as a superconductor or doping agent to enhance the superconducting properties. The findings of the most available research on cuttlefish bone have focused on its structural, morphological, mechanical, chemical, physical, biological, and physicochemical properties. Despite numerous characterization studies on cuttlefish bone, there is a notable gap in findings concerning comparing non-calcined (NCB) and calcined cuttlefish bones (CCB) at different temperatures. Such comparative analysis is crucial as it may focus on the decomposition of the pillars within cuttlefish bone, leading to the generation of CO_2 during the calcination process.

This finding holds significance in advancing our understanding of global warming due to the decomposition of $CaCO_3$ in marine life waste, such as dead coral, sea shells, and cuttlefish bone. To address marine life waste, utilization of the waste (cuttlefish bone) as a nanocomposite will be implemented. However, the characterization of this waste has been systematically conducted to assess its potential for diverse applications as nanocomposites.

2. Materials and Methods

2.1. Sample preparation of NCB.

Cuttlefish bones collected from Tok Jembal Beach (5˚24'27"N 103˚05'46"E) were stored at room temperature. Notably, all the collected samples were generally in good shape with only minor exterior flaws. Subsequently, the cuttlefish bone samples were washed and dried for two days in a controlled laboratory dryer at 30°C. This ensured that the samples remained uncontaminated while being dried at a temperature consistent with the surrounding

environment. After drying, the samples were crushed into small pieces and ground using a granite mortar and pestle until fine powder consistency. (as depicted in Figure 1). The fine powder was kept in a vial and stored in desiccators to avoid air and moisture exposure to the sample.

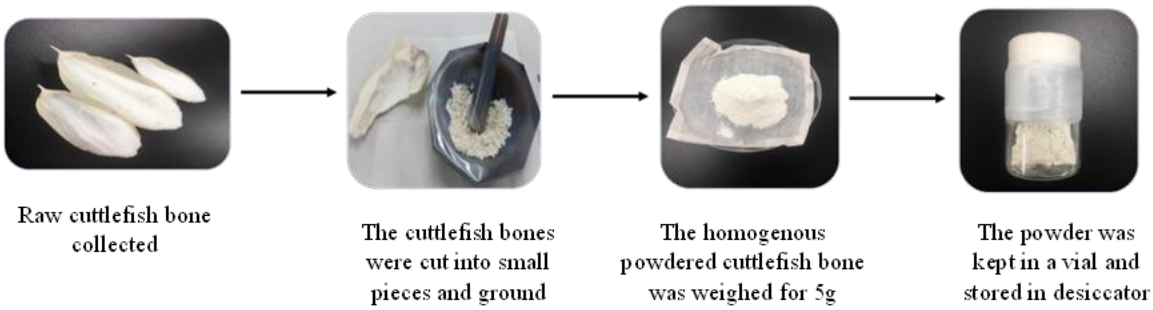

Figure 1. The procedure of preparation of the cuttlefish bone.

2.2. Sample preparation of CCB.

During the sample preparation, NCB powder (5g) was precisely weighed and placed in the furnace under controlled and optimum conditions (Carbolite Gero HTF 17 & HTF 18, United Kingdom). The calcination process was set at the temperatures of 30°C to 350°C, 30°C to 700°C and 30°C to 900°C for about 36 hours, respectively. Extended calcination periods contribute to achieving enhanced purity and homogeneity in the resulting calcium oxide. This is particularly crucial in industrial processes, where the quality of the calcium oxide affects the final product's characteristics. The controlled heating treatment was conducted at a rate of (2°C/min) with a cooling rate of (1°C/min). After the calcination process, the samples were labeled based on the maximum heating temperature, denoted as NCB, 350°C (350°C CCB), 700°C (700°C CCB) and 900°C (900°C CCB), respectively.

2.3. Thermogravimetric analysis (TGA).

Thermogravimetric Analysis (TGA) was conducted to identify thermal degradation and organic matter within the samples. While using a (Mettler Toledo TGA/DSC, Switzerland) instrument, the thermostability of the cuttlefish bone particles was investigated at a heating range from 30°C to 900°C [11]. During the analysis, 20mg of cuttlefish bone powder was placed in a platinum pan and subjected to a heating rate of 10°C/min under a dynamic oxygen flow maintained at 50 mL/min. The percentage of residue mass was recorded to estimate the mass loss of the sample following the heating process.

2.4. Scanning electron microscope with energy dispersive X-ray analysis (SEM-EDX).

The morphology of the cuttlefish bone was analyzed using SEM-EDX (Tescan Vega, Czech Republic) for elemental composition analysis on the selected area at magnification of 500 and 2000 [12]. The sample preparation involved spreading the cuttlefish bone powder on the carbon tape and blowing it to achieve a smooth surface of the powder. To obtain better imaging for the surface and cross-section, the fractured pellets and powder were coated with an ultra-thin coating of gold for 5 minutes before analyzing the samples to increase the thermal conduction and enhance the secondary electron detected by SEM. The samples were subjected to SEM with an acceleration voltage of 10 keV and 30pA. The elements of the samples were analyzed using EDX from the selected area at a magnification of x10 000.

2.5. X-ray Diffraction (XRD) analysis.

The crystalline phase of NCB, 350°C CCB, 700°C CCB, and 900°C CCB was carried out using XRD (Rigaku Mini Flex II, Japan) to evaluate the crystallite size of cuttlefish bone [12]. For this analysis, 0.3g of cuttlefish bone powder was placed on an acetone-cleaned 0.2 mm deep glass slide (sample holder) and then transferred to the XRD machine. The crystalline samples were evaluated at 30kV with a diffraction angle of 5 to 70, 2θ degrees and a λ wavelength of 1.54Å at a scanning rate of 2°/min. The Cu-Kα radiation was used, which corresponds to the X-ray wavelength. The XRD spectra of the samples were analyzed using search-match analysis and the following (1) and (2) equations [2].

The crystallinity index was determined using the following equation for each sample.

$$CI(\%) = \frac{I_{cry} - I_{ams}}{I_{cry}} \times 100 \quad (1)$$

where CI refers to the crystallinity index (%), I_{cry} refers to the maximum intensity, and I_{ams} refers to the intensity of the amorphous material between the peaks at an angle. The crystallite size was determined in accordance with the Scherrer equation,

$$crystallite\ size\ (nm) = \frac{k\lambda}{\beta\ cos\ \theta} \quad (2)$$

where k is the Scherrer constant (0.94), λ indicates the X-ray radiation wavelength, whereas ß indicates the full width at half-maximum (FWHM) of the diffraction peak, and θ indicates the Bragg corresponding angle.

2.6. Fourier transform infrared (FTIR) spectroscopy analysis.

FTIR spectroscopy (Bruker, Germany) was employed to determine the chemical properties molecular analysis, and characterize the presence of organic and mineral phases in NCB, 350°C CCB, 700°C CCB, and 900°C CCB [13]. For the analysis, a fine powdered material was placed in the mortar and ground with the pestle for one minute. At the same time, a small amount of powdered cuttlefish bone sample was placed on the cleaned tip before initiating the FTIR scanning process. The materials were recorded using an attenuated total reflectance (ATR) spectrometer for solids with a diamond crystal. Spectra were recorded in the range of 4000–400cm^{-1} with a resolution of 1cm^{-1}, and 32 scans for each sample were obtained during the analysis.

3. Results and Discussion

The characterization of cuttlefish bone was conducted using SEM, XRD, FTIR and TGA to investigate the structural, morphology, and thermal of NCB and CCB. Figure 2 shows the powder of NCB, 350°C CCB, 700°C CCB and 900°C CCB.

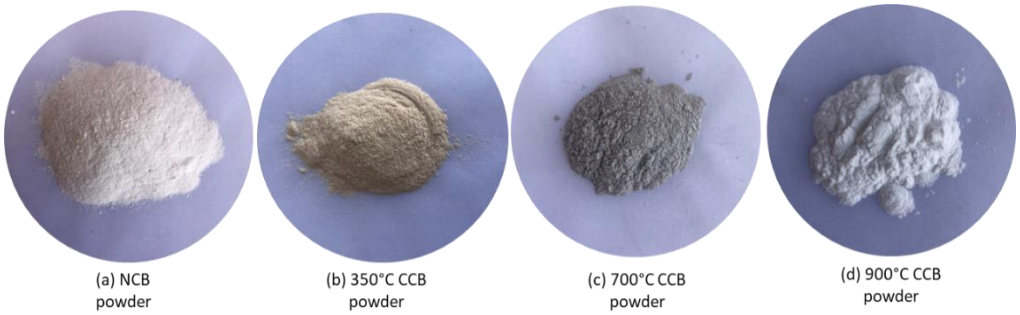

Figure 2. Calcination of cuttlefish bone at different temperatures.

The morphology of the samples showed different color characterization due to organic and water components rapidly decomposing at temperatures exceeding 500°C. Bones, which are mostly made of $CaCO_3$, undergo chemical and structural changes. Based on the figure, the powder illustrates the changes in color due to the calcination process at different temperatures. The NCB powder shows a slightly yellow color, and the 350°C CCB became brownish, while at 700°C, the CCB shows a darker greyish color. A transition from brown to black indicates a fully carbonized state of $CaCO_3$ [14]. On the other hand, at 900°C, the color of the powder becomes whiter compared to the NCB. The color changes of all powder can be attributed to the decomposition of carbon dioxide and moisture content during the calcination process. According to Mohadi *et al*. [15], greater calcination temperatures resulted in the production of more metal oxide (solid white powder) and whiter color. Suwannasingha *et al*. [16], determined that 900°C was the ideal temperature for the degradation of $CaCO_3$. Cuttlefish bone requires high temperatures to generate optimal CaO. The darker powder obtained at low temperatures indicates that cuttlefish bone powder has not completely decomposed.

3.1. Thermogravimetric analysis(TGA).

Figure 3 depicts the thermogravimetric curve analysis of cuttlefish bone powder. Based on the results, 3 stages were obtained. Stage 1 represents the degradation process, where the loss of moisture and evaporation of water started at around 36°C and went to 124°C. Whereas Stage 2 indicates the decomposition of organic matter took place at around 276°C until up to 360°C, which resulted in 0.13% weight reduction [17], and the final stage (Stage 3) illustrates the complete thermal decomposition of aragonite of the cuttlefish bone occurred as the $CaCO_3$ turned into calcium oxide (CaO) and carbon dioxide (CO_2) [16] at the temperature range of 580°C to 750°C with the weight loss of over 1.88%, suggesting that major decomposition of the NCB occurred at 580°C.

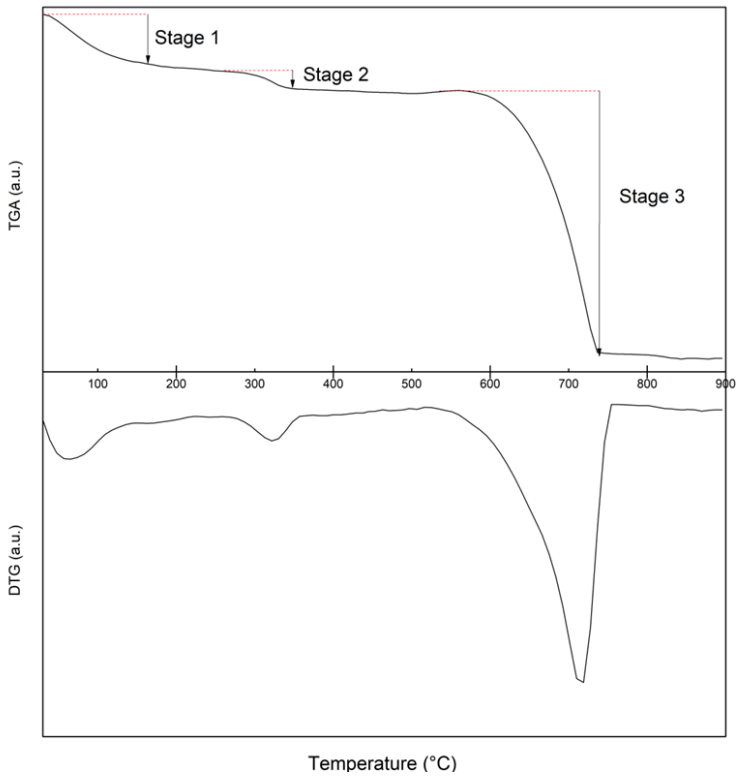

Figure 3. Thermogravimetric analysis graph of NCB.

Calcination is a heating process that may transform marine-derived $CaCO_3$ into CaO. A breakdown process is carried out at high temperatures below the melting point without using any chemicals. The most significant aspect of the process is the calcination temperature, which is often determined by the type of $CaCO_3$ or other compounds that are provided before calcination. In addition, it has also been reported that at calcination temperature, which is more than approximately 400°C of calcination, the aragonite polymorph form was converted to calcite [18].

3.2. Scanning electron microscope(SEM).

Figure 4 shows the morphology of NCB, 350°C CCB, 700°C CCB, and 900°C CCB at magnifications of 2000 and 500, respectively. The analysis observed that the microstructure of cuttlefish bone powder was found in heterogeneous shapes and varied from fine to large-size flaky form for NCB and 350°C CCB [19]. From the figure, the grain size for the NCB, 350°C CCB, 700°C CCB, and 900°C CCB were 580µm, 610µm, 453µm and 682µm respectively. The grain sizes were varied for all samples. On the other hand, the microstructure for 700°C CCB and 900°C CCB showed less dense texture compared to NCB and 350°C CCB. Additionally, extended calcination durations have an impact on the CaO flake and compact structures, causing them to begin agglomerating and to seem less regular in size and shape [20]. The individual particles were encouraged to aggregate generally by the rise in calcination temperature. The existence of the pores can be seen clearly because of grain degradation that might be affecting the connectivity of the grain when the temperature increased to 900°C CCB [21]. According to Ferraz *et al*. [1], the microstructure of cuttlefish bone has pore sizes in the range of 100-400µm and ~93% of porosity. The release of CO_2 during thermal decomposition may be influenced by these non-compact and flaky textures, which can make it difficult for internal CO_2 diffusion to control the decomposition rate [22].

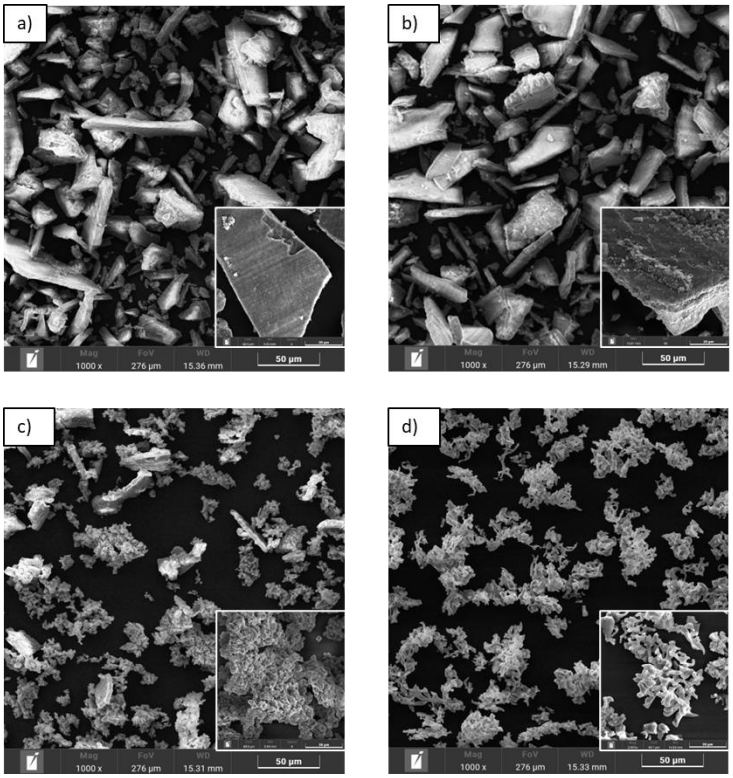

Figure 4. Micrograph of SEM at a magnification of 2000 **a**) NCB; **b**) 350°C CCB; **c**) 700°C CCB; **d**) 900°C CCB.

In order to elucidate the decomposition event of the CCB, SEM-EDX was conducted, where investigation on the molecular structure and elements of NCB and CCB was done to compare the elements content of NCB and CCB after the calcination process. Based on Figure 5 (a) and (b), the lamella structure of the NCB and the CCBs varied depending on the temperature of calcination, where the average size of the 50 selected lamella was found within the range of approximately between 124µm and 178µm for NCB and 350°C CCB, respectively. Interestingly, the lamella structures changed at the region of the bones (NCB and CCB), which are typically in the range of 200 and 600µm [23]. Other than that, the channeled architecture was completely preserved but not at a higher temperature (900°C). According to Lee *et al*. [24], higher temperatures, and lower heating duration approximately at 2 hours to 3 hours would not destroy the architecture of the lamella. But as in this study, the duration of the calcination process was 36 hours at 700°C and 900°C, the lamella structure of cuttlefish bone was destroyed. This calcination event can be attributed to the decomposition of aragonite at 750°C, as stated in TGA. Thus, it showed that the calcination duration affected the destruction of the lamella architecture of cuttlefish bone.

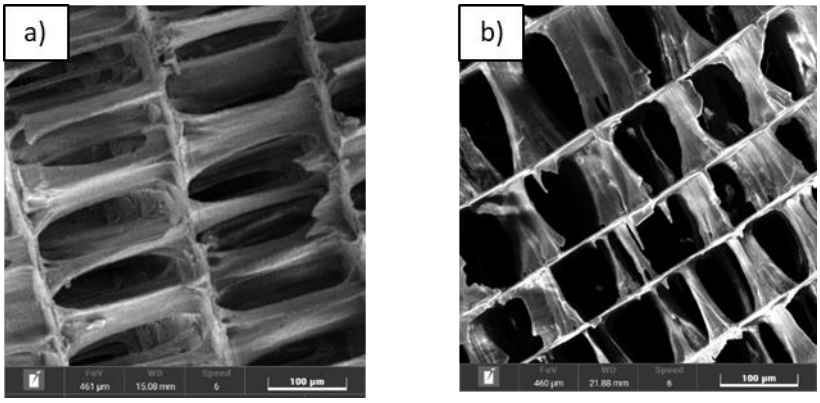

Figure 5. Micrograph of SEM at a magnification of 500 **a**) Microstructure of NCB; **b**) Microstructure of 350°C CCB.

Furthermore, a comparison of element contents in NCB and CCB and the percentage losses of some elements during the calcination process using SEM-EDX analysis could relate to the incidence of CCB's lamella size reduction (section 3.2). This study has shown that the elemental composition of Calcium (Ca), Carbon (C), and Oxygen are the major elements in the NCB and CCB specimens. Besides, minor elements such as Magnesium (Mg), Sodium (Na), Potassium (K), Rubidium (Rb), Barium (Ba), and Strontium (Sr) were abundantly found in NCB and CCB (as depicted in Table 1). All elements of 900°C CCB showed major percentage losses compared to other samples. Oxygen has the highest weight percentage compared to other elements related to the oxygen content in all samples. Oxygen at 350°C CCB slightly increased up to 52.91wt. % before decreased down to 49.12 wt. % for 900°C CCB. Furthermore, it seems that the weight percentage of all elements except calcium decreased as the temperature increased. The weight percentage for calcium increased as the temperature increased, similar to the previous study [25]. Based on the research done by Suwannasingha *et al*. [16], magnesium promotes the physical strength of marine shells by forming calcium and magnesium carbonate, which are major components of the exoskeleton structure. Thus, most marine shells, including cuttlefish bone, contain magnesium.

Table 1. EDX analysis of cuttlefish bone ($CaCO_3$) elements of NCB, 350°C CCB, 700°C CCB and 900°C CCB.

CB	Elements (wt. %)								
	O	Ca	C	Na	Rb	Sr	Ba	Mg	K
NCB	51.62	34.79	8.99	3.19	0.37	0.31	0.31	0.31	0.11
350°C CCB	45.79	42.91	6.67	2.85	0.67	0.54	0.28	0.22	0.07
700°C CCB	52.91	40.17	4.32	1.31	0.22	0.34	0.41	0.24	0.08
900°C CCB	49.12	46.80	3.22	0.34	0.20	0.22	0.00	0.07	0.03

3.3. X-ray diffraction (XRD).

Crystal structures and phases of NCB and CCB powders from 0 to 900°C were analyzed using Rigaku SmartLab software with the ICSD database to provide the crystallite size of the biomaterials. The crystallite NCB and CCB characterization have been elucidated in previous literature as catalysts and additions for other materials [9,26]. Figure 6 shows that the intensity peak of crystallinity for NCB and 350°C CCB decreased as the calcination temperature increased to 700°C CCB and 900°C CCB, which resulted in the loss of peaks.

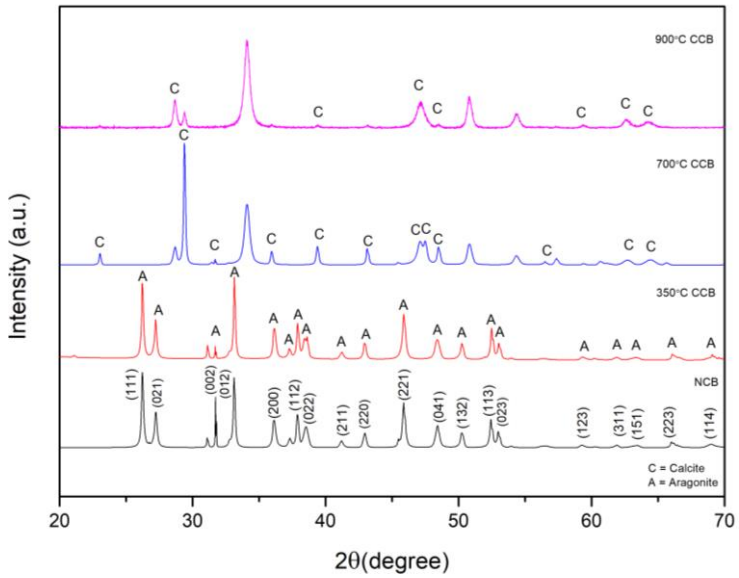

Figure 6. X-ray diffraction of NCB, 350°C CCB, 700°C CCB and 900°C CCB.

Peaks of Miller index at the degree of 26.23°, 27.27°, 31.75°, 33.11°, 36.14°, 37.86°, 38.53°, 41.25°, 42.94°, 45.89°, 48.43°, 50.24°, 52.45°, 53.00°, 59.33°, 61.92°, 63.44°,66.02° and 69.04°, corresponding to the presence of $CaCO_3$ crystallized in the aragonite phase matched with the ICSD number of 41-1475 for the standard aragonite polymorph via SearchMatch software. Meanwhile, the 700°C and 900°C CCB samples corresponded to the ICSD number of 86-2343 for the standard calcite polymorph. The results showed that the peak at (012) is the most pronounced, which indicates higher crystallinity for all samples.

Samples calcined at 900°C have the highest peak intensity of the diffraction peak at 2θ degrees of peak Miller index at (012), (112), (023), (223) and (114) at the degree of 33.10°, 37.79°, 52.96°, 65.97° and 68.75°, respectively as shown in Table 2. This difference in the 2θ intensity of the samples is due to the changing of aragonite peak intensity to calcite peaks [20]. This indicates the presence of calcite that had been transformed from aragonite by increasing the calcination temperature, which is due to the maximum decomposition of $CaCO_3$ to CaO, consistent with the results in Section 3.2 [27].

Table 2. Miller index and intensity peak of calcite phase at 900°C CCB.

Cuttlefish Bone	Calcite ($CaCO_3$)	Calcite ($CaCO_3$)	Calcite ($CaCO_3$)	Calcite ($CaCO_3$)	Calcite ($CaCO_3$)
2θ (Degree)	33.10°	37.79°	52.96°	65.97°	68.75°
Peak	012	112	023	223	114

Table 3 represents the refined lattice parameters *a*, *b*, *c* axis and unit cell volume, *V* of NCB and CCB. It shows that NCB and 350°C CCB samples are in orthorhombic structure with the lattice parameters *a*, *b*, *c* axis and unit cell volume, *V* decreased due to the conversion of $CaCO_3$ to CaO [28]. However, the structure changed to hexagonal for 700°C and 900°C CCB owing to the full decomposition of aragonite to calcite phase [20].

Table 3. Lattice parameters, *a*, *b*, *c* axis and unit cell volume, *V* for NCB and CCB.

Cuttlefish Bone	***a*** (Å)	***b*** **(Å)**	***c*** **(Å)**	**V (Å3)**
NCB	4.9623	7.9680	5.7439	227.1115
350°C CCB	4.9598	7.9641	5.7379	226.6490
700°C CCB	4.9760	-	17.4880	-
900°C CCB	4.4983	-	17.0200	-

Table 4 depicts the crystallinity index (CI) and the crystallite size (Å) for cuttlefish bone samples. The table showed that the crystallite size obtained was slightly increased for the 350°C CCB sample and then decreased as the temperature increased up to 900°C CCB. The results confirmed that the 900°C CCB has the lowest crystallite size compared to others at 23.30nm. It is believed that the decreasing crystallite size is due to changing aragonite peak intensity to calcite peaks [29]. In addition, Amoudeh *et al*. [5] stated that the grinding process causes the natural $CaCO_3$ crystal to decrease in size. The crystallite size also refers to the agglomeration of the samples according to the SEM analysis, which shows that the lower crystalline size leads to a decrease in size [30].

Table 4. XRD analysis for determining the crystallinity index (CI) and the crystallite size (***nm***) for cuttlefish bone samples.

Samples	**Crystallinity index (%)**	**Crystallite size (*nm*)**
NCB	87.09	55.52
350°C CCB	87.24	64.03
700°C CCB	81.35	44.74
900°C CCB	64.20	23.30

3.4. Fourier-transform infrared spectroscopy (FTIR).

Moreover, FTIR spectrum of NCB and 350°C CCB in Figure 7 shows a familiar spectrum profile during the temperature increment to 700°C CCB and 900°C CCB, which resulted in the decrease of cuttlefish bone peaks.

The findings correspond with the aragonite phase in Section 3.3 (Fig. 6), and the previous analysis stated by Ferraz *et al*., 2020 supported the aragonite formation. Strong aragonite structure carbonate group peaks were confirmed at 1444cm^{-1} (asymmetric stretching) due to the internal vibration mode of carbonate ions [19], 1081 (symmetric stretching), 853cm^{-1} (out-of-plane bending) and doublet at 712cm^{-1}. Small intensity bands were also noticed at 1784c m^{-1} and 1776 of NCB and 350°C CCB, which were most likely caused by a harmonic vibration referred to as OH stretching vibration [1,16]. Additionally, the presence of calcite phase was referred to the band between 712 and 871cm^{-1} in the FT-IR spectrum. The change of metastable aragonite from ambient pressure to a stable calcite with around 450°C heating can be used to explain the crystallization and phase transition of $CaCO_3$ [14].

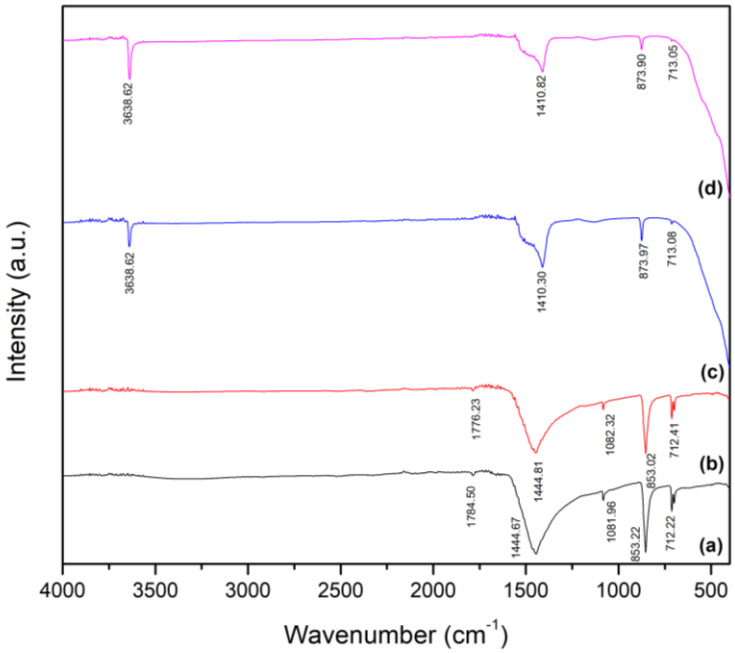

Figure 7. Fourier-transform infrared spectroscopy (FTIR) of **(a)** NCB; **(b)** 350°C CCB; **(c)** 700°C CCB; **(d)** 900°C CCB.

Cuttlefish bone structure exhibits an absorption band at 3814 cm^{-1} when heated at 700°C and 900°C. This matches the OH stretching during the adsorption of water by CaO [31]. The decreasing peak at 713 cm^{-1} in the FT-IR spectra of 700°C CCB and 900°C CCB, which may be the C-O stretching bands, revealed carbonate was missing, respectively. This illustrates the general reduction in peak intensity of the cuttlefish bone, which indicated that some functional chemical groups of the biomaterials were eliminated during heat treatment. The XRD and FT-IR results have assured the complete transformation of CaO from $CaCO_3$ at the calcination temperature of 700°C for CB and 900°C. Thus, the FTIR spectra data of the CCBs at 350°C, 700°C, and 900°C were varied due to the formation of aragonite and calcite polymorphs.

4. Conclusions

The study's findings depicted that the cuttlefish bone powder was successfully extracted from the raw cuttlefish bone waste and calcined at different temperatures. During this study, the complete conversion of cuttlefish bone from $CaCO_3$ to CaO can be achieved via the calcination process at 750°C through the solid-state method. While the crystalline structure changed from aragonite polymorph to calcite according to the XRD analysis. Morphological changes were observed, shifting from a flake-like structure to a more agglomerate structure with a decrease in the percentage of elements in EDX analysis except for Ca, which depicted an increase in percentage at higher temperatures. The results signify the possibility of cuttlefish bone as a natural precursor to generate CaO in easier and more time-saving ways that can contribute to various applications and help manage the biomass waste of cuttlefish bone. The study concluded that 900°C CCB is the optimum temperature of the cuttlefish bone and the most compatible replacement for natural CaO that can be utilized in various potential advanced applications that require nanosized CaO. Furthermore, this study helps researchers and students to plan further research on cuttlefish bone based on its properties at different temperatures to determine its reliability and compatibility in green technology applications.

Funding

This research received no external funding.

Acknowledgments

The authors would like to thank the Ministry of Higher Education, Malaysia, and the University of Malaysia Terengganu (UMT). We also would like to acknowledge the Nanophysics Laboratory of the Faculty of Science and Marine Environment for their support in conducting the research and analysis sample.

Conflict of Interest

The authors declare no conflict of interest.

References

1. Ferraz, E.; Gamelas, J.A.F.; Coroado, J.; Monteiro, C.; Rocha, F. Exploring the potential of cuttlebone waste to produce building lime. *Mater. Construccion* **2020**, *70*, e225, http://doi.org/10.3989/mc.2020.15819.
2. Sainorudin, M.H.; Abdullah, N.A.; Asmal Rani, M.S.; Mohammad, M.; Mahizan, M.; Shadan, N.; Abd Kadir, N.H.; Yaakob, Z.; El-Denglawey, A.; Alam, M. Structural characterization of microcrystalline and nanocrystalline cellulose from *Ananas comosus* L. leaves: Cytocompatibility and molecular docking studies. *Nanotechnol. Rev.* **2021**, *10*, 793–806, http://doi.org/10.1515/ntrev-2021-0053.
3. Nouj, N.; Hafid, N.; El Alem, N.; Buciscanu, I.I.; Maier, S.S.; Samoila, P.; Soreanu, G.; Cretescu, I.; Stan, C.D. Valorization of β-Chitin Extraction Byproduct from Cuttlefish Bone and Its Application in Food Wastewater Treatment. *Materials* **2022**, *15*, 2803, http://doi.org/10.3390/ma15082803.
4. Krishnan, S.; Chakraborty, K.; Dhara, S. Biomedical potential of β-chitosan from cuttlebone of cephalopods. *Carbohydr. Polym.* **2021**, *273*, 118591.
5. Amoudeh, Z.; Jalali, T.; Osfouri, S. Fabrication and characterization of $YCa_2Cu_3O_7$ superconductors using natural ($CaCO_3$) nanoparticles extracted from *Sepia pharaonis*. *Appl. Phys. A* **2020**, *126*, 25, http://doi.org/10.1007/s00339-019-3196-2.
6. Ferro, A.C.; Guedes, M. Mechanochemical synthesis of hydroxyapatite using cuttlefish bone and chicken eggshell as calcium precursors. *Mater. Sci. Eng. C* **2019**, *97*, 124–140, http://doi.org/10.1016/j.msec.2018.11.083.
7. Ressler, A.; Bauer, L.; Prebeg, T.; Ledinski, M.; Hussainova, I.; Urlić, I.; Ivanković, M.; Ivanković, H. PCL/Si-Doped Multi-Phase Calcium Phosphate Scaffolds Derived from Cuttlefish Bone. *Materials* **2022**, *15*, 3348, http://doi.org/10.3390/ma15093348.
8. Ling, X.; Osotsi, M.I.; Zhang, W.; Wu, Y.; Jin, Q.; Zhang, D. Bioinspired Materials: From Distinct Dimensional Architecture to Thermal Regulation Properties. *J. Bionic Eng.* **2023**, *20*, 873–899, http://doi.org/10.1007/s42235-022-00314-w.
9. Darwish, A.S.; Sayed, M.A.; Shebl, A. Cuttlefish bone stabilized Ag_3VO_4 nanocomposite and its Y_2O_3-decorated form: Waste-to-value development of efficiently ecofriendly visible-light-photoactive and biocidal agents for dyeing, bacterial and larvae depollution of Egypt's wastewater. *J. Photochem. Photobiol. A Chem.* **2020**, *401*, 112749, http://doi.org/10.1016/j.jphotochem.2020.112749.
10. Rial, R.; González-Durruthy, M.; Liu, Z.; Ruso, J.M. Advanced Materials Based on Nanosized Hydroxyapatite. *Molecules* **2021**, *26*, 3190, http://doi.org/10.3390/molecules26113190.
11. Kalpana, M.; Nagalakshmi, R. Effect of reaction temperature and pH on structural and morphological properties of hydroxyapatite from precipitation method. *J. Indian Chem. Soc.* **2023**, *100*, 100947, http://doi.org/10.1016/j.jics.2023.100947.
12. Yazid, H.; Achour, Y.; Kassimi, A.E.; Nadir, I.; Himri, M.E.; Laamari, M.R.; Haddad, M.E. Removal of Congo Red from Aqueous Solution Using Cuttlefish Bone Powder. *Phys. Chem. Res.* **2021**, *9*, 565–577, http://doi.org/10.22036/pcr.2021.278943.1901.
13. Hazeena, S.H.; Hou, C.-Y.; Zeng, J.-H.; Li, B.-H.; Lin, T.-C.; Liu, C.-S.; Chang, C.-I.; Hsieh, S.-L.; Shih,

M.-K. Extraction Optimization and Structural Characteristics of Chitosan from Cuttlefish (*S. pharaonis* sp.) Bone. *Materials* **2022**, *15*, 7969, http://doi.org/10.3390/ma15227969.

14. Tomano, N.; Prokaew, A.; Boonyuen, S.; Ummartyotin, S. Development of Sr/CaO catalyst derived from cuttlebone (Sepia officinalis) for biodiesel production. *J. Met. Mater. Miner.* **2020**, *30*, 40–47, http://doi.org/10.14456/jmmm.2020.5.
15. Mohadi, R.; Anggraini, K.; Riyanti, F.; Lesbani, A. Preparation Calcium Oxide (CaO) from Chicken Eggshells. *Sriwij. J. Environ.* **2016**, *1*, 32–35.
16. Suwannasingha, N.; Kantavong, A.; Tunkijjanukij, S.; Aenglong, C.; Liu, H.-B.; Klaypradit, W. Effect of calcination temperature on structure and characteristics of calcium oxide powder derived from marine shell waste. *J. Saudi Chem. Soc.* **2022**, *26*, 101441, http://doi.org/10.1016/j.jscs.2022.101441.
17. Curti, F.; Serafim, A.; Olaret, E.; Dinescu, S.; Samoila, I.; Vasile, B.S.; Iovu, H.; Lungu, A.; Stancu, I.C.; Marinescu, R. Development of Biocomposite Alginate-Cuttlebone-Gelatin 3D Printing Inks Designed for Scaffolds with Bone Regeneration Potential. *Mar. Drugs* **2022**, *20*, 670, http://doi.org/10.3390/md20110670.
18. Bin Bakri, M.K.; Rahman, M.R.; Matin, M.M.; Yurkin, Y.; Burkov, A.; Jayamani, E.; Kuok, K.K.; Yun, C.M.; Omoregie, A.I. 11 - Marine-based reinforcing materials for biocomposites. In Recycled Plastic Biocomposites, Rahman, M.R.; Bin Bakri, M.K., Eds.; Woodhead Publishing, **2022**, 229-245, https://doi.org/10.1016/B978-0-323-88653-6.00010-9.
19. Periasamy, K.; Mohankumar, G.C. Sea coral-derived cuttlebone reinforced epoxy composites: Characterization and tensile properties evaluation with mathematical models. *J. Compos. Mater.* **2016**, *50*, 807–823, http://doi.org/10.1177/0021998315581512.
20. Tagar, U.; Volpe, M.; Messineo, A.; Volpe, R. Highly ordered CaO from cuttlefish bone calcination for the efficient adsorption of methylene blue from water. *Front. Chem.* **2023**, *11*, 1132464, http://doi.org/10.3389/fchem.2023.1132464.
21. Borciani, G.; Fischetti, T.; Ciapetti, G.; Montesissa, M.; Baldini, N.; Graziani, G. Marine biological waste as a source of hydroxyapatite for bone tissue engineering applications. *Ceram. Int.* **2023**, *49*, 1572–1584, https://doi.org/10.1016/j.ceramint.2022.10.341.
22. Soisuwan, S.; Phommachant, J.; Wisaijorn, W.; Praserthdam, P. The Characteristics of Green Calcium Oxide Derived from Aquatic Materials. *Procedia Chem.* **2014**, *9*, 53–61, http://doi.org/10.1016/j.proche.2014.05.007.
23. Mao, A.; Zhao, N.; Liang, Y.; Bai, H. Mechanically Efficient Cellular Materials Inspired by Cuttlebone. *Adv. Mater.* **2021**, *33*, 2007348, http://doi.org/10.1002/adma.202007348.
24. Lee, J.-B.; Maeng, W.-Y.; Koh, Y.-H.; Kim, H.-E. Porous Calcium Phosphate Ceramic Scaffolds with Tailored Pore Orientations and Mechanical Properties Using Lithography-Based Ceramic 3D Printing Technique. *Materials* **2018**, *11*, 1711, http://doi.org/10.3390/ma11091711.
25. Ismail, R.; Cionita, T.; Shing, W.L.; Fitriyana, D.F.; Siregar, J.P.; Bayuseno, A.P.; Nugraha, F.W.; Muhamadin, R.C.; Junid, R.; Endot, N.A. Synthesis and Characterization of Calcium Carbonate Obtained from Green Mussel and Crab Shells as a Biomaterials Candidate. *Materials* **2022**, *15*, 5712, http://doi.org/10.3390/ma15165712.
26. Anitta, S.; Sekar, C. Voltammetric determination of paracetamol and ciprofloxacin in the presence of vitamin C using cuttlefish bone-derived hydroxyapatite sub-microparticles as electrode material. *Results Chem.* **2023**, *5*, 100816, http://doi.org/10.1016/j.rechem.2023.100816.
27. Zuliantoni, Z.; Suprapto, W.; Setyarini, P.H.; Gapsari, F. Extraction and characterization of snail shell waste hydroxyapatite. *Results Eng.* **2022**, *14*, 100390, http://doi.org/10.1016/j.rineng.2022.100390.
28. Bhagyaraj, S.; Al-Ghouti, M.A.; Khan, M.; Kasak, P.; Krupa, I. Modified *os sepiae* of *Sepiella inermis* as a low cost, sustainable, bio-based adsorbent for the effective remediation of boron from aqueous solution. *Environ. Sci. Pollut. Res.* **2022**, *29*, 71014–71032, http://doi.org/10.1007/s11356-022-20578-3.
29. Khaenamkaew, P.; Manop, D.; Tanghengjaroen, C.; Ayuthaya, W.P.N. Effect of Temperature Treatment on Electrical Property, Crystal Structures and Lattice Strains of Precipitated $CaCO_3$ Nanoparticles. *Mat. Res.* **2019**, *22*, http://doi.org/10.1590/1980-5373-MR-2019-0461.
30. Khine, E.E.; Koncz-Horvath, D.; Kristaly, F.; Ferenczi, T.; Karacs, G.; Baumli, P.; Kaptay, G. Synthesis and characterization of calcium oxide nanoparticles for CO_2 capture. *J. Nanopart. Res.* **2022**, *24*, 139, http://doi.org/10.1007/s11051-022-05518-z.

31. Balu, S.k.; Bargavi, P.; Chitra, S.; Kannan, S.; Ramadoss, R.; Andra, S. Morphological evaluation of HAp nanostructures and its shape-dependent protein adsorption study. *Mater. Lett.* **2023**, *331*, 133491, http://doi.org/10.1016/j.matlet.2022.133491.